This is a peer-reviewed, accepted author manuscript of the following article:
Zhang, Y., Yin, M., Zeng, Q., Wang, T., & Wang, R. (2020).
Theoretical and experimental investigation of variable stiffness finger seal.
Tribology Transactions . https://doi.org/10.1080/10402004.2020.1730532

Theoretical and experimental investigation of variable stiffness finger seal

Yan-chao Zhang [a] *, Ming-hu Yin [a] *, Quan-ren Zeng [a, b], Ting Wang [a], Rui Wang [a]

a School of Mechanical and Precision Instrument Engineering, Xi'an University of Technology, Xi'an, China.

b Department of Design, Manufacture and Engineering Management, University of Strathclyde, Glasgow, UK.

* Correspondence: zhangyanchao@xaut.edu.cn Tel.: +86-135-7187-4962

Abstract: Finger seal is a flexible and dynamic contact seal, many researches and experiments have proved its great application potential in aviation engines, gas turbines, and other equipment. However, the contradiction between hysteresis leakage and wear life in the design and the initial installation condition of finger seal seriously affect the integrated performance design effect. A variable stiffness finger seal is investigated in the present study to resolve the aforementioned problems, and the influence of initial installation condition is considered. First, a theoretical model of the finger seal is established to calculate the hysteresis characteristic and contact pressure between finger feet and rotor. The performances of the variable stiffness finger seal and traditional involute curved finger seal are compared to confirm the advantages of the variable stiffness finger seal. The results show that the initial conditions such as rotor structure and support bearing clearance have important influence on the accuracy of finger sealing performance calculation. In addition, the variable stiffness structure improves the hysteresis characteristic of the finger seal with virtually no loss of wear life under low pressure differential and reduces the hysteresis rate by more than 50%. Under high pressure differential, the variable stiffness structure reduces the average contact pressure by more than 25%. Therefore, the leakage and wear performance of the finger seal are simultaneously improved by the variable stiffness structure. This characteristic does not change with increase in rotor excitation. This indicates that the variable stiffness finger seal provides good synthetic performance and high dynamic adaptability to random operating conditions.

Keywords: Variable stiffness; Finger seal; Hysteresis leakage; Initial installation condition; Durability.

INTRODUCTION

A dynamic seal device is an important component of aviation engines, gas turbines, and other high-speed rotating equipment such as ground-based combustion engines, water turbines, etc. Existing studies show that when fabricating such equipment, improvements and developments in advanced sealing technology are considerably more significant than improvements to the performance of other parts. Advanced seal technology is an effective method of improving the leakage and wear performance of engines with large income and less cost. For example, the thrust of gas turbines can be increased by 4%–6% and their fuel ratio can be reduced by 1%–2.62% through advanced seal technology **[1-3]**.

Finger seals are a kind of dynamic and contact seal can be used to seal parts in aviation engines, main-shaft bearing chambers in gas turbines, and top gas energy recovery units in blast furnaces **[4-6]**. Finger seal is proposed on the basis of brush seal. As a flexible contact seal, finger seal and brush seal are much better than labyrinth seal. In the static condition, the leakage performance of finger seal is lower than that of labyrinth seal; while in the dynamic condition, the finger seal has a comparable leakage in comparison with brush seal. However, the finger seal can effectively avoid the problem of brush wire fracture and bristle tip melting while retaining the flexible characteristics of brush seal, and the manufacturing cost is relatively low. Preliminary experimental results show that the leakage of finger seal is 20%–70% less than that of labyrinth seal **[7]**. Furthermore, the experimental results of NASA's Glenn Research Center show that the average leakage can be reduced by 50% after replacing the labyrinth seal with finger seal in the typical parts of engine. This decreases the fuel

consumption of engine by 0.7%–1.4% and running cost by 0.35%–0.7% **[8-10]**. However, the investigation and engineering applications of the finger seal are still hindered owing to the contradiction between leakage and wear in design **[11]**.

A large number of studies have been conducted on finger seals in recent years. Hendricks et al. used numerical simulation to analyze the performance of finger seal and compared the analysis results with those of brush seal and labyrinth seal. The results revealed that the leakage of finger seal was almost same as that of brush seal and considerably less than that of labyrinth seal **[10]**. Arora et al. proposed a low hysteresis finger seal with a pressure balanced chamber. In this type of finger seal, a chamber was placed between an aft cover plate and a downstream finger element; high-pressure gas was directed into the chamber to balance pressure and reduce hysteresis; the pressure balanced chamber can considerably reduce hysteresis, but it also leads to a high risk for leakage **[8]**. Wang et al. studied the dynamic performance of C/C composite finger seal; although it has better wear resistance than super alloy materials, but its axial size has increased by 4 times or even more, and its manufacturing cost has increased greatly **[12-13]**. Chen et al. analyzed the mechanical properties of finger seal with various curves (such as logarithmic spiral and involute), and proposed an active control optimization method for the design of shape-curve to improve the hysteresis and stiffness of finger seal **[14-15]**. Zhang et al. used a multi-objective optimization method to optimize the structural parameters of finger seal through game theory **[16]**. Braun et al. researched the thermo-fluids seal behavior of padded finger seal by using numerical simulation method; in this work, the displacement transmissibility, gas stiffness and temperatures influence were studied, and the results showed

that the proposed geometry provides a satisfactory lifting capability for the fingers under specific conditions; however, how to ensure the stability of the gas film under variable rotating speed, and how to ensure the expected gas film gap under the influence of complex temperature conditions and machining errors are the key problems for padded finger seal **[17-18]**.

Various methods have been proposed to resolve the contradictions between the hysteresis and wear life of finger seal, but improvements to the effect remain limited. Although the non-contact finger seal proposed by the researchers on the basis of contact configuration finger seal can better alleviate this contradiction, the dynamic film stability problem existing in the non-contact finger seal, and the processing cost is high, so its application is often constrained.

Finger seal design follows the principle of ensuring its leakage level is small, while meeting the requirements of wear life. However, in the finger seal design, it is found that increasing stiffness through the control wire is the main way to reduce the hysteresis leakage. But, the increase in stiffness will bring about an increase in the sealing/rotor contact pressure and increase the wear. This feature is the contradiction in design. To alleviate the contradiction between hysteresis and wear caused by the structural design of finger seal, Su et al. attempted to use arbitrary curve structures to improve the design contradiction by expanding the search space of a curve control point and to prevent the constraints of the structure generated by the customized shape curve; however, to reduce the computational time in the study, the curve parameters of the finger seal were limited and only a freeform curve with an upper concave configuration was optimized **[19]**. Li et al. used the Stackelberg strategy to optimize the shape curve of finger seal in free space, and a new finger seal with an upper concave curve was

proposed; furthermore, a comparison of the dynamic performances of the traditional involute curved finger seal and logarithmic spiral curve finger seal showed that the finger seal with the upper concave curve had a small hysteresis characteristic when the rotor run-out is large, and its contact pressure was almost simultaneously improved; this finding provided a new idea for the design of the shape curve of finger seal; however, there was no specific analysis of the structure of finger feet in the study, and therefore, further improvement of the axial structure of finger seal is required **[20]**.

Based on the dynamic operating characteristic of the finger seal and actual engineering design requirements, the present works designs a variable stiffness curve structure for the finger seal and studies its performance, and the results are verified through experiments. With this variable stiffness structure, the deformations of finger beams occur in the low damping region at small rotor run-out; while at large rotor run-out, the deformation region transfers to the high damping region, which provides large restoring stiffness to control hysteresis. Therefore, the variable stiffness curve structure can resolve the contradiction between the hysteresis leakage and wear life of the finger seal effectively.

VARIABLE STIFFNESS FINGER SEAL

The structure of variable stiffness finger seal is similar to that of traditional involute curved finger seal. As shown in Figures 1 and 2, the variable stiffness finger seal is composed of a stack of finger elements and forward and aft cover plates, and it is clamped by rivets. Each element includes several flexible finger beams placed symmetrically along the circumferential direction. An element rotates relative to its adjacent elements because the gaps between fingers

can be covered. The finger elements are in close contact with a rotor to eliminate gas leakage. However, unlike the traditional involute curved finger seal, the finger beams of the variable stiffness finger seal adopt an upward concave curve and the width of the finger beams increases gradually from the inner circle to the root circle; the specific structure of its finger beam means the closer the finger beam to the root circle, the larger its stiffness is, which leads to variable stiffness along the curve profile of finger beam. Thus, when the rotor run-out is small, the deformation of finger beam mainly concentrates at the part closer to the finger feet, where the width of finger beam is small and its stiffness is also small, that is benefit to reduce the contact pressure between the finger feet and rotor; as the rotor run-out increases, the deformation area of finger beam also increases and extends towards the root circle gradually, where the width of finger beam is large and its stiffness is also large, that can enhance the elastic restoring force to reduce hysteresis leakage. Thus, as the periodical change of rotor run-out, the finger seal can self-adapt to rotor run-out owing to the variable stiffness structure, which is effective for decreasing the contact pressure and hysteresis leakage during operation.

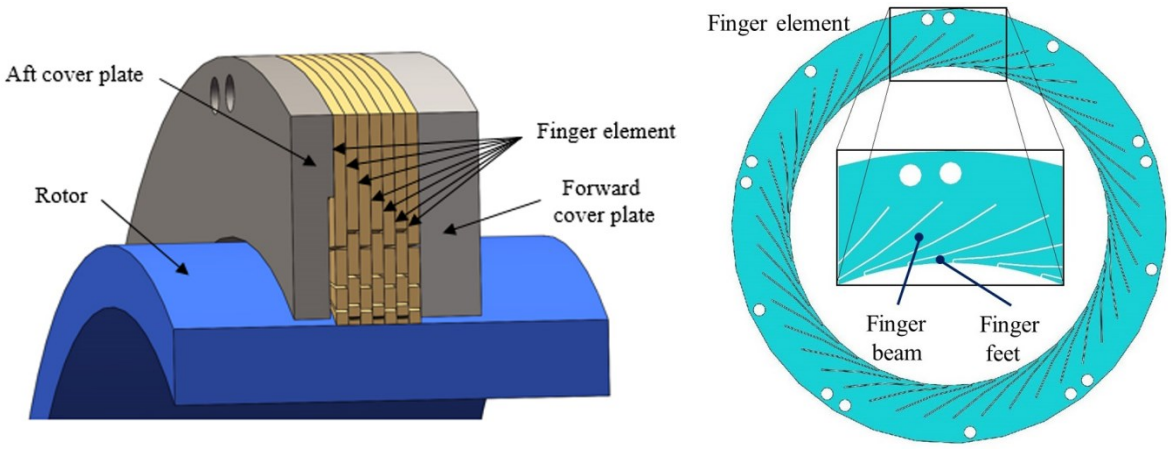

(a) variable stiffness finger seal (b)finger element

Figure 1. Constitution and parameters of variable stiffness finger seal

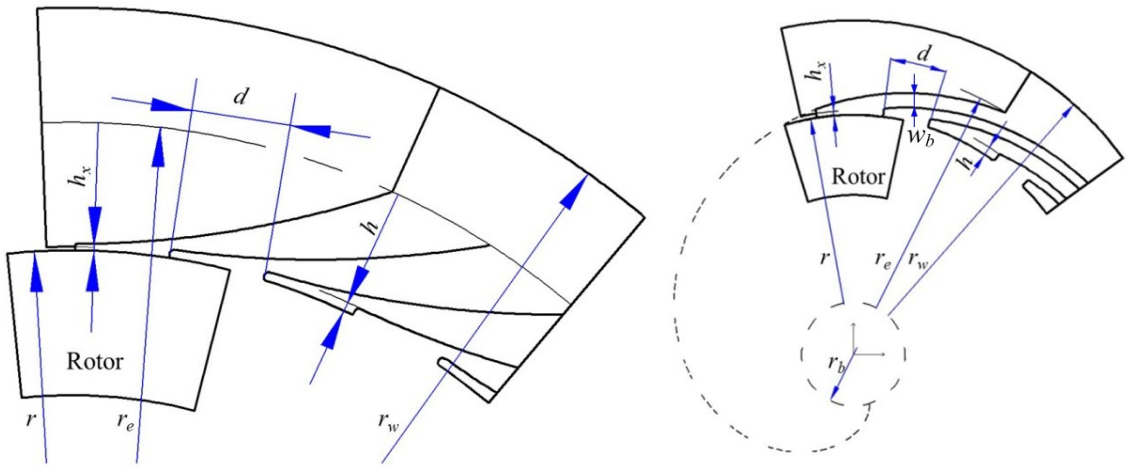

(a) variable stiffness finger seal (b) traditional involute curved finger seal

Figure 2. Parameters of variable stiffness finger seal and traditional involute curved finger seal

PERFORMANCE ANALYSIS MODEL OF FINGER SEAL

Simulation model

Owing to the cyclic symmetrical structure of the finger seal in the circumferential direction and its cyclic superimposed structure in the axial direction, a simplified model is established to simulate the operation of the finger seal, as shown in Figure 3. The model includes part of the rotor, part of the aft cover plate and part of two layers of finger elements along the axial direction; the finger element far from the aft cover plate is adjacent to the upstream (called upstream finger element), while the finger element contacting with the aft cover plate is adjacent to the downstream (called downstream finger element); along the circumferential direction, the upstream finger element includes one complete finger and two half fingers, while the downstream finger element only includes two complete fingers to cover the gaps between adjacent fingers of upstream finger element. The Grid partition unit type is 8 node hexahedron SOLID 185, and the total number of grid divisions is 23287. The materials and physical performance parameters of the model are shown in Table 1.

The following boundary conditions are imposed, as shown in Figure 4:

a) The outer circular surfaces of the finger elements and the back face of the aft cover plate are fixed (surfaces 1 and 2).

b) Symmetric cyclic boundary conditions are imposed on the sections of the rotor, finger elements, and aft cover plate (surfaces 3 and 7); an axial constraint is imposed on the rotor (surfaces 4).

c) The pressure differential between upstream and downstream (Δp) is imposed at the front face of the first finger element (surfaces 6), the pressure differential ranges from 0.1 to 0.4 MPa.

d) Contact pairs are imposed at the contact area between the finger feet and rotor, the contact area between the second finger element and aft cover plate, and the contact areas between adjacent finger elements.

e) The mass of the rotor is unbalanced owing to the material defect and machining error, which introduces radial run-out during rotation. Owing to the rotor run-out and friction among finger elements or between finger elements and cover plates, hysteresis clearance occurs between the finger feet and rotor, which leads to the hysteresis leakage. Therefore, the simulation of rotor run-out is important for the performance analysis of the finger seal. In this study, dynamic rotor run-out is simulated using the sinusoidal displacement excitation function introduced in Ref **[21]**, which is expressed as

$$\begin{cases} y(t) = \dfrac{\delta n}{n^*} \sin(\dfrac{n\pi}{30} t) & n \le n^* \\ y(t) = \delta \sin(\dfrac{n\pi}{30} t) & n > n^* \\ n^* = \dfrac{30}{\pi} \sqrt{\dfrac{Mg}{m_e}} \end{cases} \tag{1}$$

Where, $y(t)$ is the displacement excitation of the rotor, n is the rotating speed of the rotor, and δ is the radial clearance of a supporting bearing; n^* is the "specific" rotating speed of the rotor; M is the mass of rotor; m_e is the unbalance amount of rotor; g is the gravitational acceleration. In the paper, to facilitate the comparison between the theoretical and experimental results, the theoretical calculations are based on the experimental structural conditions; thus, according to the model and accuracy class of the aviation angular contact bearing used in the test rig, δ is set as 0.09 mm; and according to the structure and dynamic balance amount of the rotor used in the test rig, n^* is set as 9500 r/min.

As mentioned above, because of the friction among finger elements or between finger elements and cover plates, there are amplitude and phase differences between the rotor run-out and displacement response of the finger seal, which lead to the hysteresis leakage. Therefore, the transient simulation is used to analyze the performance of the finger seal. During the transient simulation, the distance between all nodes on the finger feet and rotor can be measured at each time step. Then, the average of these distances can be defined as the leakage clearance of the finger seal at a time step. The leakage clearance in a complete cycle can be obtained using this method, and the leakage rate of the finger seal can be obtained by utilizing hydromechanics theory.

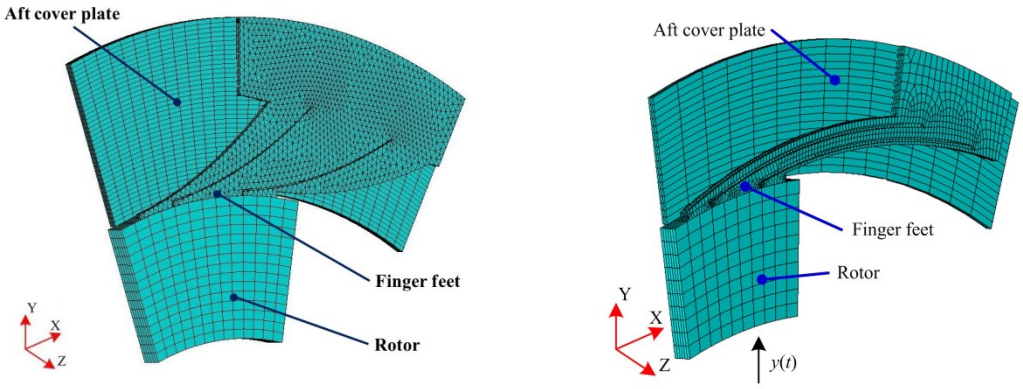

(a) variable stiffness finger seal (b) traditional involute curved finger seal

Figure 3. Finite element analysis model of finger seal

Table 1 Materials and physical performance parameters of the model

	Materials	Elastic modulus ($\times 10^{11}$Pa)	Poisson's ratio	Densities (g/cm^3)
Finger element	GH605	2.31	0.286	9.13
cover plate	2Cr13	2.14	0.346	6.35
Rotor	40CrNiMoA	209	0.295	7.85

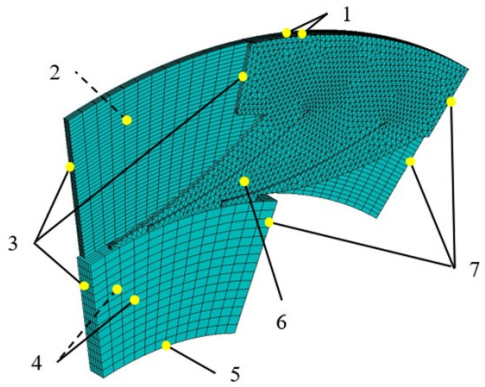

1and 2--Fixed Constraints; 3 and 7--Symmetric circular constraints; 4 Axial constraints; 5 Rotor displacement excitation; 6 Upstream and downstream pressure differential.

Figure 4. The boundary conditions of finger seal

Calculation of leakage rate for finger seal

The dynamic response of the finger seal is different from that of the rotor in terms of amplitude and phase. This creates leakage clearance between the finger feet and rotor and leads to the leakage in the finger seal. Therefore, through the finite element simulation of the finger seal, the leakage can be calculated by the difference between the rotor excitation and the

dynamic response of finger seal. Besides, It is known that the initial position of the rotor is eccentric because of supporting bearing clearance; owing to this, the bottom finger beams are preloaded and the upper finger beams do not contact the rotor. Therefore, initial installation condition may influence the shape and change law of the leakage clearance between the finger feet and rotor. Thus, the initial installation condition between the finger seal and the rotor has an important influence on leakage clearance, which should be considered in the simulation. To reveal the influence of initial installation condition, the contact state between the finger feet and rotor can be divided into several regions; the performance of entire circle finger seal can be obtained with the compound of the results in all regions. In this paper, during the simulation analysis of finger seal, according to the deformation characteristics of finger seal, in order to consider the influence of deformation on cyclic symmetry characteristics, and considering the balance between the amount and accuracy of calculation, the simulation model of finger seal is divided into four regions (upper region, left region, lower region and right region, as shown in Figure 5). In Figure 5, the white imaginary lines are the boundaries between adjacent regions; points 1, 2, 3 and 4 are the middle points of the four regions respectively; points A, B, C, D are the boundary points (intersection points of boundaries and finger feet) of the four regions respectively; according to the deformation characteristics, the number of finger beams in the upper and lower regions is 11, and the number of finger beams in the left and right regions is 10. In the calculation of the upper and lower regions, the difference between the deformation of the finger feet in the middle region (the calculation model of middle region includes the finger foot in the middle point and the adjacent finger feet) and the farthest regions on both

sides (the calculation model of farthest region includes the finger foot in the boundary point and the adjacent finger feet) is approximately 6.5%; while for the left and right regions, the difference between the deformation of the finger feet in the middle region and the farthest regions on both sides is approximately 5.8%. In order to eliminate calculation error, when calculating the deformation of finger feet in each region, the average value of the deformation of all finger feet is used as the final value of the deformation of the finger feet in this region.

As shown in Figure 5, according to initial installation condition, the radial distance between point 1 in the upper region and the rotor is set as supporting bearing clearance. The distance between point 2 (or 4) in the left middle region (or right middle region) and the rotor is set as 0. Point 3 in the lower region is contact with the rotor, and the preformation of the finger beams equals supporting bearing clearance.

The performance analysis model shown in Figure 2 is used to calculate the leakage rate of each region. Finally, the leakage rate of the entire finger seal can be obtained as the summation of the leakage rates in the four regions **[21]**, and it can be expressed as

$$Q = \sum_{j=1}^{4} N_j \frac{\Delta t}{T} \sum_{i=1}^{k} \beta \Delta l \frac{\Delta p \rho h_{ij}^3}{12 \eta L} \tag{2}$$

where k is the number of time steps in one motion cycle (k = 20); N_j is the number of circular symmetrical structures in the j^{th} region; Δt is the time step ($\Delta t = 60/nk$); T is the motion cycle of the rotor ($T = 60/n$); Δp is the pressure differential between upstream and downstream; ρ is the density of sealed fluid; Δl is the arc length of leakage clearance long the circumferential direction; h_{ij} is the height of leakage clearance at the i^{th} time step in the j^{th} region; L is the axial thickness of finger seal; η is the dynamic viscosity of sealed fluid; β is the leakage coefficient,

it is introduced in the equation to express the effects that cannot be considering in the theoretical model (such as assembly or manufacturing error, speed or pressure fluctuation and so on, especially the backlash leakage between adjacent finger elements or finger elements and cover plates caused by the surface roughness and the deformation under pressure differential.), the leakage coefficient can be obtained through a static leakage experiment and theoretical calculation, and its value is the ratio of the static test leakage value to the theoretical leakage calculation results. With the modified theoretical leakage calculation results, the effect which is difficult to estimate can be considered, and the leakage rate of finger seal can also be predicted.

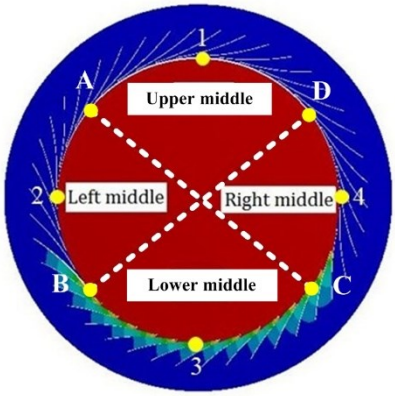

Figure 5. Region division of finger seal

THEORETICAL RESULTS AND DISCUSSION

In this study, to compare the performances of the variable stiffness finger seal and traditional involute curved finger seal, the structure optimizations of these seals are carried out based on the self-developed method introduced in Ref **[22-23].** The structural parameters of the seals after optimization are listed in Table 2. Using the performance analysis model presented in this paper, their sealing performances are calculated under various pressure differentials,

rotating speeds, and supporting bearing clearances.

Table 2 Structural parameters of finger seal

Parameters	Symbol	Units	Involute	Variable stiffness
Radius of rotor	r	mm	40	40
Outer radius of finger beam	r_w	mm	55	55
Clearance	d	mm	0.2	0.2
Height of finger feet	h	mm	0.7	0.4
Number of finger beams	m	--	42	42
Thickness of finger elements	t	mm	0.2	0.2
Root radius of finger beam	$\mathrm{r_e}$	mm	48	48
Downstream protection height	$\mathrm{h_x}$	mm	0.45	0.45
Radius of base circle	$\mathrm{r_b}$	mm	0.008	--

In this paper, some physical quantities (such as leakage clearance, hysteresis rate, contact pressure, etc.) are calculated based on the simulation results of the above finite element model, which should be defined here. Figure 6 shows the schematic diagram of the working process for finger seal; when the finger seal is working, its finger feet could move up and down under the action of contact force and the elastic restoring force of fingers; when the finger feet drop down, they could not return to their original positions rapidly due to the frictions between the adjacent finger elements or finger elements and cover plates caused by the pressure differential between upstream and downstream, which leads to the hysteresis leakage. In the simulation process, the contact pressure of all nodes between the finger feet and rotor can be obtained, define the average of these contact pressures as the average contact pressure of finger seal; While the rotor is moved to its original position, due to the hysteresis, there is a distance between finger feet and rotor, measure the distances of all nodes, the distances are the leakage clearances; define the average of these leakage clearances as the average leakage clearance of finger seal; define the ratio of average leakage clearance to the rotor run-out as the hysteresis

rate of finger seal; define the average of hysteresis rates at each time in a complete cycle as the average hysteresis rate of finger seal.

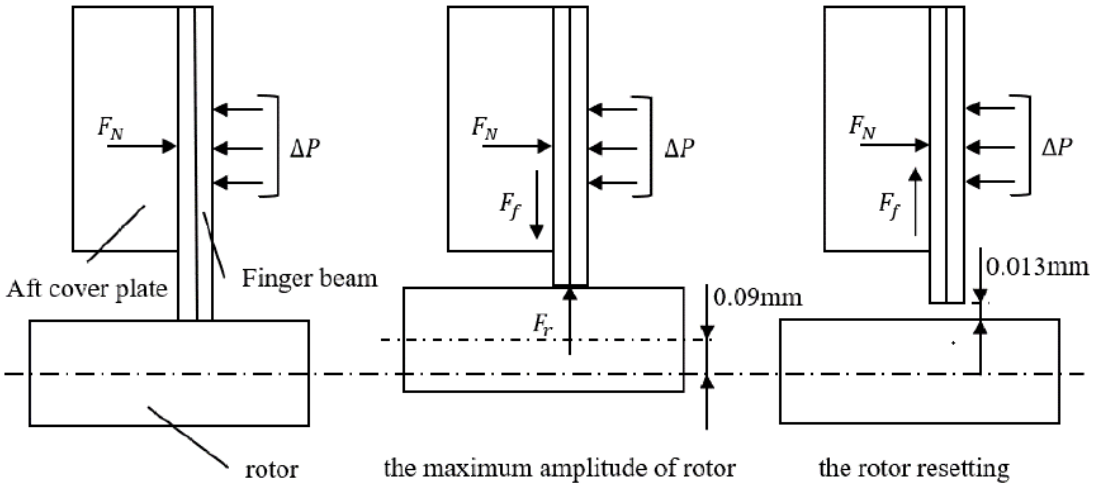

Figure 6. The schematic diagram of the working process for finger seal

Figure 7 shows the radial displacements of the variable stiffness finger seal and traditional involute curved finger seal at the maximum amplitude of rotor run-out under n = 9500 r/min, Δp = 0.2 MPa, and δ = 0.09 mm. It can be seen that because of the variable stiffness structure, as the rotor moves towards the finger, the deformation of the finger beam increases, then the stiffness of the finger increases. Thus, the major deformation area of the variable stiffness finger seal is smaller than that of the involute curved finger seal and is closer to the finger feet; it means that the area acted with frictions of variable stiffness finger seal is also smaller than that of the involute curved finger seal, which also means the hysteresis leakage caused by frictions is decreased. Table 3 provides the average contact pressure and average hysteresis rate of the two types of finger seals in a complete cycle. As shown in the table, the average contact pressure and hysteresis rate are reduced by 23% and 50% respectively, when the variable stiffness structure is used. This proves the advantage of the variable stiffness finger seal.

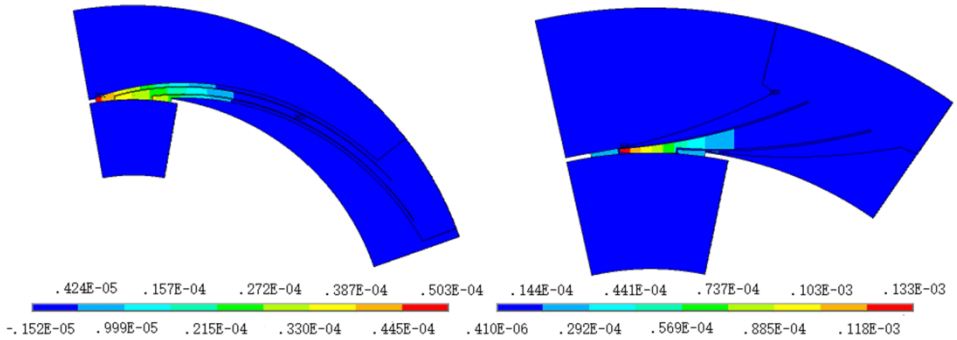

Figure 7. Radial displacement results of finger seal (n=9500r/min, Δp=0.2MPa, δ=0.09mm)

Table 3 Average hysteresis rate and contact pressure of finger seal

Parameters	Involute	Variable stiffness
Hysteresis rate（%）	80.2	39.6
Average contact pressure（MPa）	0.5725	0.4386

Figure 8 shows the calculation results of the displacement response and hysteresis clearance of the two types of finger seals in a complete cycle under various pressure differentials at n = 9000 r/min and δ = 0.085 mm. It is seen that the displacements between the finger feet and rotor of the finger seals change with the rotor run-out. When the rotor moves up along the radial direction, the finger feet and beams are pushed up; whereas when the rotor moves down, the finger feet cannot keep up with the rotor immediately because of the effect of frictions, and hysteresis is produced. However, with the variable stiffness structure, the hysteresis clearance of the variable stiffness finger seal is considerably smaller than that of the involute curved finger seal.

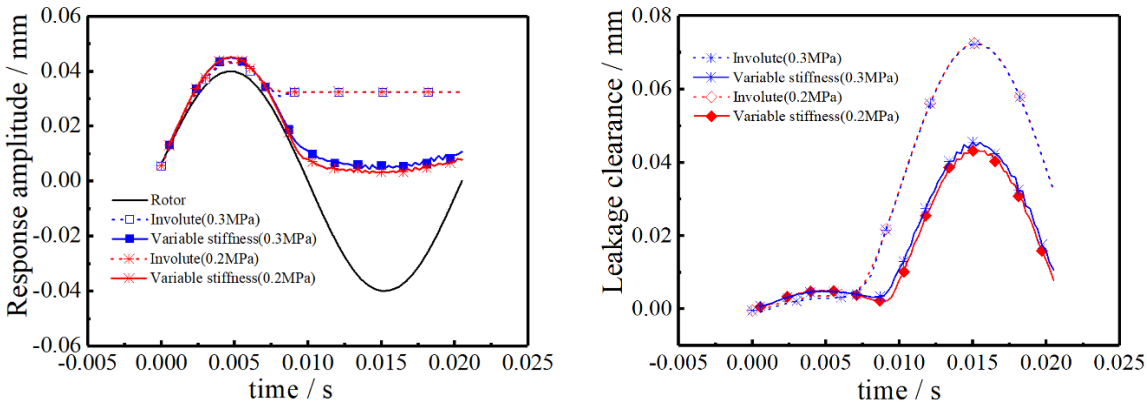

(a) Displacement response (b) Leakage clearance

Figure 8. Displacement response results of finger seal（δ=0.085mm）

Figure 9 shows the calculation results of the displacement response and hysteresis clearance of the two types of finger seals in a complete cycle at δ = 0.16. It can be seen that, compared with the results shown in Figure 8, the amplitude of rotor run-out increases to 0.08 mm with increase of supporting bearing clearance. Thus, the hysteresis clearance of the two types of finger seals increases. This indicates that initial installation condition has considerable influence on the performance of finger seals. However, the variable stiffness finger seal still exhibits smaller hysteresis clearance. This proves that the variable stiffness finger seal can provide higher sealing performance under various initial installation conditions.

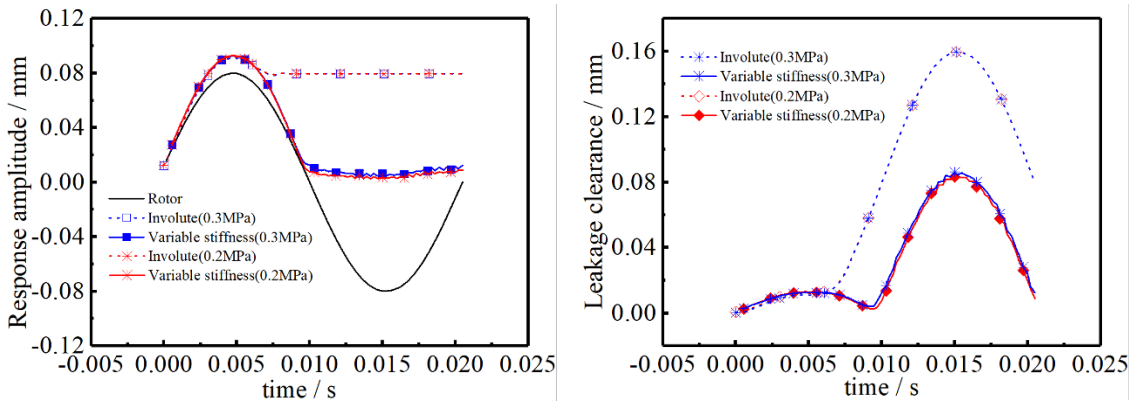

(a) Displacement response (b) Leakage clearance

Figure 9. Displacement response results of finger seal（δ=0.16mm）

To evaluate the sealing performance of variable stiffness finger seal and involute curved finger seal under random operating conditions, Figure 10 and Figure 11 show the average hysteresis rates and average contact pressures for the two types of finger seals with rotating speed under various pressure differentials. According to equation (1), the amplitude of rotor run-out increases as the enhance of rotating speed; and as the increase of pressure differential, the pressures among adjacent finger elements or between finger elements and cover plates increase, so the frictions among adjacent finger elements or between finger elements and cover plates increase consequentially. For the traditional involute finger seal, due to the equal width (the width of finger beam along the normal direction of involute, called normal width, which is dimensioned as "w_b" in Figure 2b) design of its finger beam, the stiffness of its finger beams can't adapt the change of rotor run-out or frictions caused by the change of rotating speed or pressure differential; hence, with the increase of rotating speed and pressure differential, the average hysteresis rate and average contact pressure of the traditional involute curved finger seal both increase. However, the variable stiffness finger seal can self-adapt to the increase of rotor run-out owing to the variable stiffness of finger beams; therefore, its average hysteresis rate does not increase but decreases with the increase of rotating speed (Figure 10); in addition, its average hysteresis rate becomes smaller than that of the involute curved finger seal after the rotating speed increases to 5000 r/min. The average contact pressure of the variable stiffness finger seal also increases with the increase of pressure differential (Figure 11); but its average contact pressure is considerably smaller than that of the involute curved finger seal when the pressure differential is 0.3 MPa and 0.4 MPa. The above theoretical analysis indicates that with

the self-adaptive capacity of the variable stiffness structure, the variable stiffness finger seal can balance hysteresis and wear to achieve high synthetic performance. Furthermore, under high speed or high pressure conditions, the variable stiffness finger seal provides excellent sealing performance that cannot be achieved by the traditional involute curved finger seal.

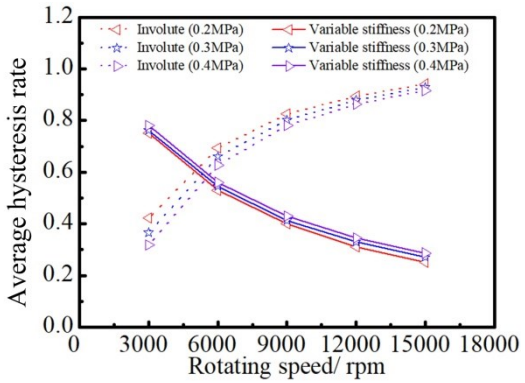

Figure 10. Rotating speed and pressure differential affect on leakage of involute finger seal

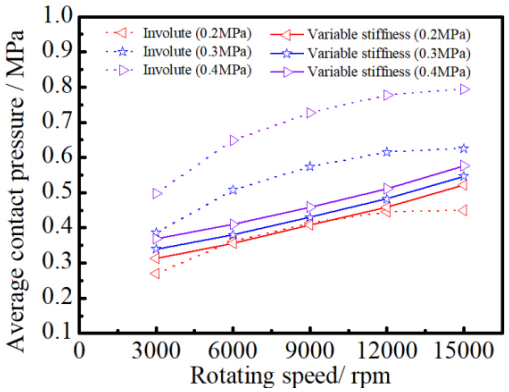

Figure 11. Result of average contact pressure between rotor and finger feet

The dynamic operating condition of the finger seal at different positions along the circumferential direction under the displacement excitation of the rotor is different at the same moment in time. To analyze the dynamic operating condition of the variable stiffness finger seal in different regions along the circumferential direction, Figure 12 shows the calculation results of the displacement response of the finger feet at specific positions in different regions when the rotating speed is 5000 r/min and the pressure differential is 0.2 MPa. For visual analysis and calculation, the excitation and response curves in the graph are treated as follows: the corresponding excitation curves of the rotor are given for each region and the response curves of the finger feet remove the phase difference at each specific position. In this manner, the difference between the displacement response of the finger feet and the displacement excitation of the rotor at each specific position at a moment is the size of the leakage clearance

at this moment.

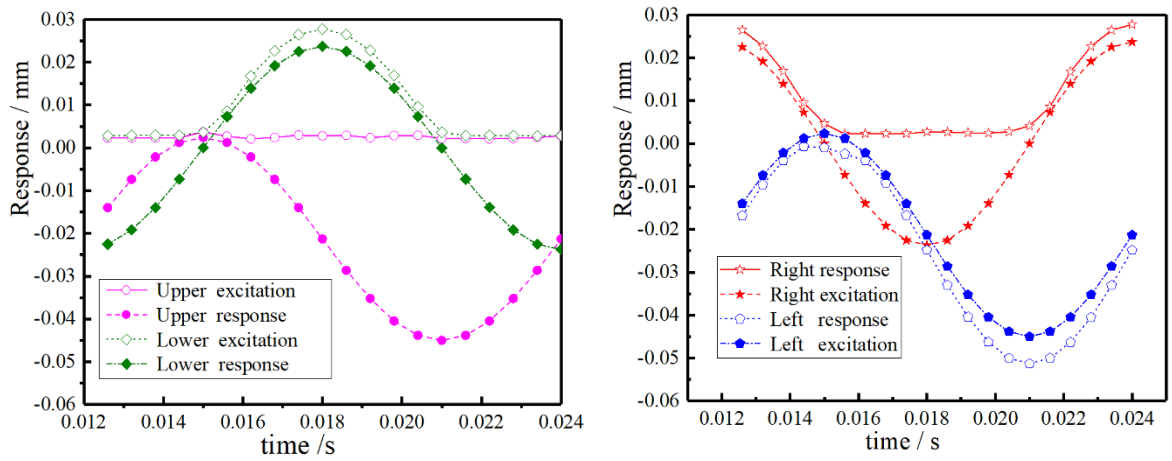

(a) The rotor excitation and displacement responses in the upper and lower regions (b) The rotor excitation and displacement responses in the left and right regions

Figure 12. The dynamic response of finger seal in different circumferential regions (Δp=0.2 MPa, n =5000 r/min)

Figure 12 shows that the displacement response of the finger seal at the upper specific position is a straight line close to zero. This is because the rotating speed is lower than the "specific" rotating speed. Owing to this, the rotor only has small contact with the upper region of the finger seal only at the largest run-out amplitude. Thus, there is almost no displacement in the upper specific position. On the contrary, the phenomenon of following the rotor motion at the lower specific position of the finger seal is the most evident, and the reason is related to the compression contact state between the lower specific position and rotor at the beginning. At this time, the finger seal is always in the compression state during the entire operating process because the variable stiffness finger seal exhibits good dynamic followability. The displacement response of the finger seal at the right middle specific position intersects with the displacement response at the left middle specific position and is similar to it; however, there is a phase difference of 180°. This is related to the difference of 180° between the two positions.

The finger seal is in normal contact with the rotor at left middle and right middle specific positions. Therefore, its characteristics are similar to those shown in Figure 6. The analysis results of the dynamic performance of the variable stiffness finger seal in the circumferential direction indicate that hysteresis leakage performance must be treated differently. The effect of different dynamic operating conditions in the circumferential direction is considered owing to the difference in the dynamic operating state in different regions in the circumferential direction.

EXPERIMENTAL INVESTIGATION

Test rig and test sample

To evaluate the sealing performance of the variable stiffness finger seal and verify the performance analysis model established in this paper, a self-developed dynamic sealing test rig is used to carry out the performance tests of the variable stiffness finger seal. The construction of the test rig and test unit is shown in Figure 13.

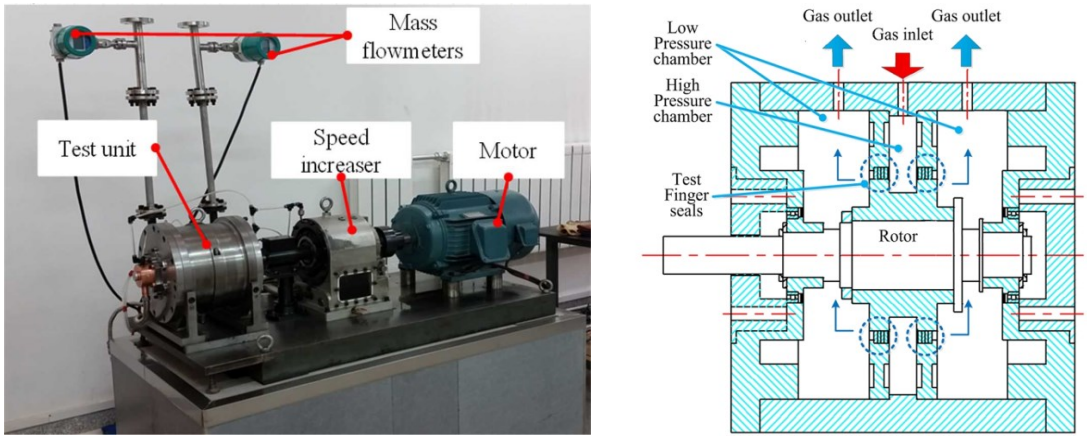

(a) Test rig (b) Test unit

Figure 13. The test-bed for high-speed dynamic seal

The test rig is driven by a three-phase asynchronous motor with a rated speed of 5000

r/min. The motor is connected with the rotor of the test unit with couplings and a speed increaser, which makes the highest rotating speed of the finger seal test unit reach 30000 r/min. A vortex gas compressor supplies high-pressure gas for the experiments, and the pressure of the gas can be adjusted through a pressure regulating valve. In order to eliminate the influence of the oil mist in the shaft bearing cavity that may leak the lubricant in the leaking gas on the leakage measurement results, the tester adopts a double-layer design; the low-pressure cavity air hole is opened at the bottom of the inner layer of the tester, and at the same time, a vent hole is set in the middle of the outer shell of the tester, and the external flow meter is measured. In the experiments, the high-pressure gas flows into the high-pressure chamber of the test unit, leaks into two adjacent low-pressure chambers through two variable stiffness finger seals, and exhausts through two vents at the bottom. The vents are connected to two mass flow meters, which measure the leakage rates of the two variable stiffness finger seals.

In the test unit, the two low-pressure chambers are separated from the high-pressure chamber by two variable stiffness finger seals with the same structure, which is shown in Figure 14. The material of the test variable stiffness finger seal is GH605 alloy steel. The material of the sealing runway is 40CrNiMoA alloy steel, and its surface is coated with hard chrome to enhance wear performance. The structural parameters of the test variable stiffness finger seal are given in Table 2.

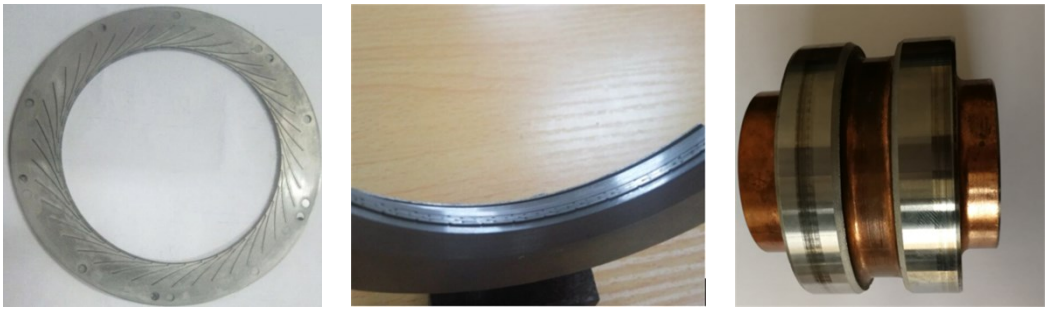

(a) Finger element (b) Assembled finger seal (c) sealing runway

Figure 14. Test samples of variable stiffness finger seal

Experimental procedure

As mentioned above, the leakage rates of the two test finger seals are measured by two mass flow meters connected with the two vents at the bottom of the test unit. To minimize the measurement error caused by manufacture and assembly, the average of the two measuring results are defined as the final result of each test.

In the experiments, leakage tests are carried out at four pressure differentials (0.1 MPa, 0.2 MPa, 0.3 MPa, and 0.4 MPa). First, static leakage tests (the rotor is not rotating) are carried out at each pressure differential. Dynamic tests (the rotor is rotating at various speeds) are performed after the static leakage tests. In the dynamic tests, the rotating speed is increased as follows: 0 r/min, 3000 r/min, 5000 r/min, 7000 r/min, 9000 r/min, and 12000 r/min. Then, it is decreased to zero. The speed loading method is shown in Figure 15. Furthermore, to evaluate the operating stability of the variable stiffness finger seal, a durability test is carried out for 10 h at a pressure differential of 0.2 MPa and a rotating speed of 9000 r/min.

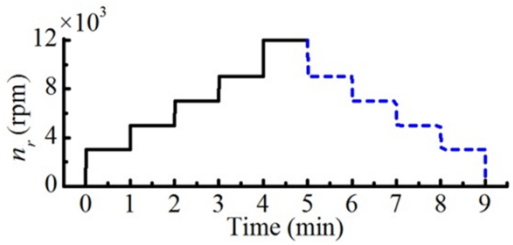

Figure 15. The speed loading method

Experimental results

The leakage rates of the variable stiffness finger seal obtained in the static tests are shown in Figure 16. As it is known, in the processing and manufacturing, due to the flexible contact design of the finger seal, it is difficult to measure the gap between the test pieces after assembled; so the contact state between the finger seal and the sealing runway is controlled by the tolerance between the finger seal and sealing runway (apply transition fit in general), it means that there is no leak gap in theory. However, due to the influence of the pressure differential between upstream and downstream in the static test, the contact state of the finger seal changes, which cause gap leakage and become the main path of static leakage. As it is known, the radial gap due to hysteresis is the main cause of leakage in the dynamic work of finger seal, and it is also the theoretical basis of performance design and calculation. But in the static state, there's no hysteresis, the main leakage path of finger seal just is the backlash leakage (because of the surface roughness and the deformation of finger elements under pressure differential, there are backlashes between adjacent finger elements or finger elements and cover plates, which causes backlash leakage of finger seal). Thus, as the pressure differential increases, the deformation of finger elements increases, so the backlash leakage increases gradually (as shown in Figure 16). While under the dynamic state, the hysteresis leakage arises, but the backlash leakage won't fade away but also play an important role; according to the experiment sample's machining accuracy, it clearance between the finger feet and rotor is 0.005 mm; at Δp = 0.3 MPa, the static leakage rate is only 0.23 g/s in theory, but

the experimental leakage rate reaches 6.68 g/s; that is primarily because the tested variable stiffness finger seal only has 7 layers of finger elements and its axial thickness is only 1.4 mm, so the axial deformation of the finger elements under the pressure differential is large, which leads to such serious backlash leakage. Thus, the backlash leakage plays an important role in the leakage of finger seal no matter static or dynamic state, but it is difficult to be considered in the theoretical model, that' why the leakage coefficient (β) is introduced in the leakage rate calculation model of finger seal (equation 2 at section "Calculation of leakage rate for finger seal") to predict its dynamic sealing performance. According to the static tests in this paper, the leakage coefficient is set as , the theoretical results shown in Figure 16 to 19 are all modified with the leakage coefficient.

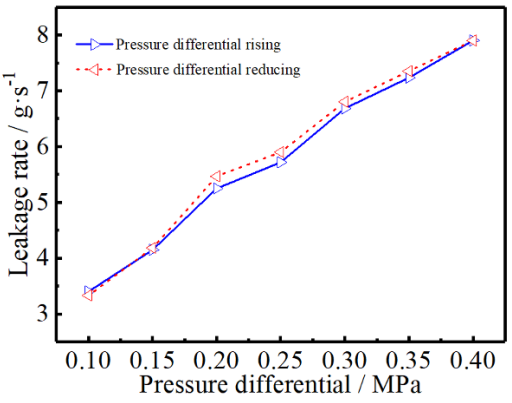

Figure 16. Static leakage rates under the different pressure differential

Figure 17 shows the change in leakage performance of variable stiffness finger seal with rotating speed under different pressure differentials under dynamic state. The dynamic leakage rate under different pressure differentials decreases gradually with increase in rotating speed. This is because the unbalanced force against the weight of the rotor increases with rotor speed, the upward "float" of the rotor is promoted, and the "closure" degree of leakage clearance is increased, thereby reducing the leakage rate of the finger seal. The leakage rates of the finger

seal show basically the same trend with change in rotating speed at the reducing speed stage. This is the same trend as that observed in the theoretical analysis. This fully validates the rationale of the leakage calculation method based on the initial operating condition of the rotor and the condition of the circumferential region. Besides, according to the dynamic test results, at the initial raising speed stage (n=3000rpm~5000rpm), the change of leakage rate with rotating speed is quite different from the general law (at n=5000rpm~12000rpm, the leakage rate decreases with the increase of rotating speed; but under n=3000rpm~5000rpm, with the increase of rotating speed, the change of leakage rate is small or even increases at Δp=0.3MPa); that may be due to the difference of backlash leakage caused by different deformation of finger seal under different pressure conditions.

The experiments of traditional involute curved finger seal with the similar structural parameters of the tested variable stiffness finger seal didn't carry out intentionally. Thus, the leakage performance of a previous involute curved finger (its radius of rotor and outer radius of finger beam are 33mm and 47mm respectively, which have a certain difference with that of the tested variable stiffness finger seal can only be gave in Figure 18. According to the experimental results shown in Figure 17 and 18, although there's a certain difference between the previous involute curved finger and the tested variable stiffness finger seal, their change laws of leakage rate via rotating speed or pressure differential are quite accordant; furthermore, the leakage rate of the previous involute curved finger is smaller than that of the tested variable stiffness finger seal; but it should be noticed that, the radius of rotor of the previous involute curved finger is smaller than that of the tested variable stiffness finger seal, which means its

circumferential length of leakage clearance is also smaller than that of the tested variable stiffness finger seal. Thus, it can be predict that the variable stiffness finger seal has a considerable or even better sealing performance under the similar structural and operating conditions. The further theoretical and experimental research on the difference between the variable stiffness finger seal and other types of finger seal will be carried out in the authors' future work.

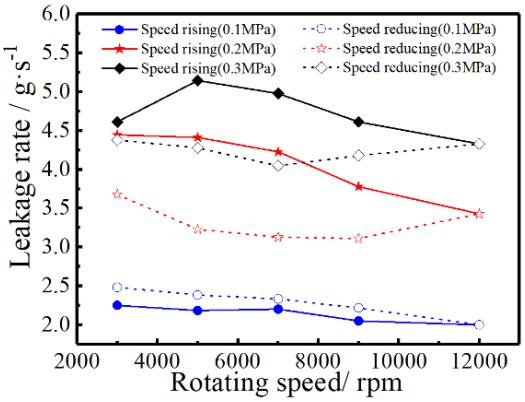

Figure 17. The dynamic leakage test results of variable stiffness finger seal (r=40mm, r_w=55mm)

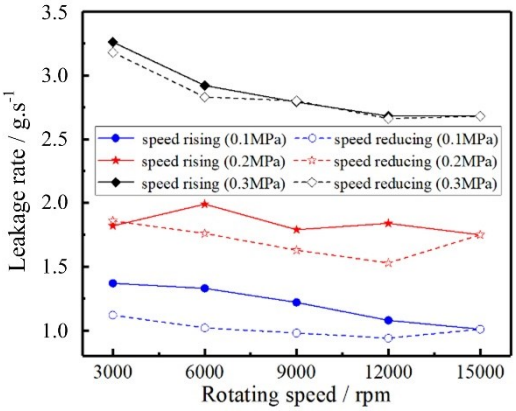

Figure 18. The dynamic leakage test results of involute finger seal (r=33mm, r_w=47mm)

Furthermore, it can be seen from the experimental results that the leakage rate of the variable stiffness finger seal (Figure 17) at the reducing speed stage is larger than that at the raising speed stage under a pressure differential of 0.1 MPa. This is caused by the hysteresis characteristic of the finger seal. That is, the radial run-out amplitude of the rotor decreases with rotating speed. However, the finger seal cannot completely follow the rotor resetting, and "suspension" occurs at a higher position compared to the run-out amplitude of the rotor at this time owing to the friction between the finger element and aft cover plate or among the finger elements. This phenomenon leads to the gradual separation of the finger seal from the rotor, resulting in larger leakage clearance. This shows that leakage increases with decrease in

rotating speed. This phenomenon is also consistent with the theoretical analysis. However, this phenomenon is not observed in the experiments when the pressure differential increases to 0.2 MPa and 0.3 MPa. This is consistent with the phenomenon of lower contact pressure under higher pressure differential shown in Figure 11. This is mainly due to the special structure of the variable stiffness finger seal. Another reason is that as the backlash leakage of the finger seal increases with the pressure differential. There is backlash leakage flow between the finger elements and aft cover plate and among the finger elements, and frictional resistance is significantly reduced. The over reset phenomenon appears with decrease in rotating speed. This shows that the leakage rate at the reducing speed stage is smaller than at the raising speed stage. This characteristic has not been observed in the leakage experiment of the traditional involute curved finger seal. This indicates that the variable stiffness finger seal has a good characteristic under random change in rotating speed.

A durability experiment was carried out for 10 h to evaluate the dynamic operating stability of the variable stiffness finger seal. The experimental results of the leakage performance of the variable stiffness finger seal under a pressure differential of 0.2 MPa and a rotating speed of 9000 r/min are shown in Figure 19. There is a certain degree of fluctuation at the initial stage, which may be caused by initial contacting wear of rough contact surfaces in the running-in stage. At the latter stable stage, the overall leakage performance is extremely stable during the durability experiment, except for a slight fluctuation caused by the fluctuation of the air supply system. This demonstrates the dynamic operating stability of the variable stiffness finger seal. Besides, for the experimental requirement of another project, and

considering the efficiency and cost, the durability experiment of finger seal in this paper was carried out with a carbon ring seal concurrently; the photos of sealing runway before the durability experiment weren't taken, so there is a black trace on the left sealing runway in the Figure 14c.

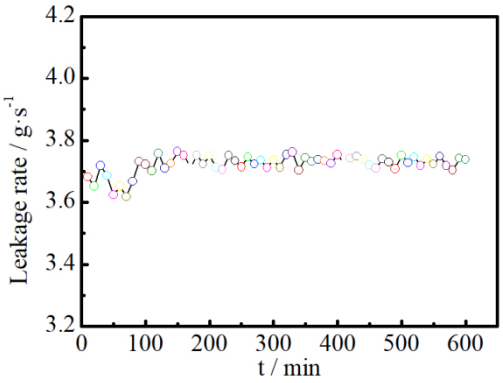

Figure 19. Durability test results(P=0.2MPa, n=9000r/min)

Figure 20 compares the experimental results to the theoretical analysis of variable stiffness finger seal leakage under dynamic conditions. It can be seen from the figure that the theoretical analysis is in good agreement with the experimental results. The reason for the backlash leakage of finger seal is mainly due to the rough contact between the finger elements and aft cover plates, as well as the deformation caused by the finger seal under the action of the upstream and downstream pressure differential. The finger seal has a multi-layer structure, so this backlash leakage has porous leakage characteristics similar to brush seal, and the Ref **[24]** also studied this characteristic. Because the influence of the sealing deformation of finger caused by the pressure differential in the upstream and downstream under static leakage conditions, the leakage performance of the backlash is more obvious. However, under dynamic working conditions, due to the high-frequency beating of the rotor, the high-frequency beating of the pointed beam leads to the high-frequency beating of the pointed beam, and the high-

frequency beating of the pointed beam acts as a shear damper to the leaking fluid in the backlash. Therefore, the leakage of the backlash of the finger seal is no longer obvious under the dynamic leakage conditions compared to the static conditions. The leakage rates obtained through theoretical analysis are slightly different from the experimental results. The main reasons for this can be deduced as follows: (a) the backlash leakage in the dynamic tests; (b) the theoretical motion trail of the rotor exhibits error compared to the actual trail. Based on the above comparison, the established performance calculation method of the variable stiffness finger seal can reflect the actual operating condition of the finger seal and provide an effective reference for the performance design of the finger seal.

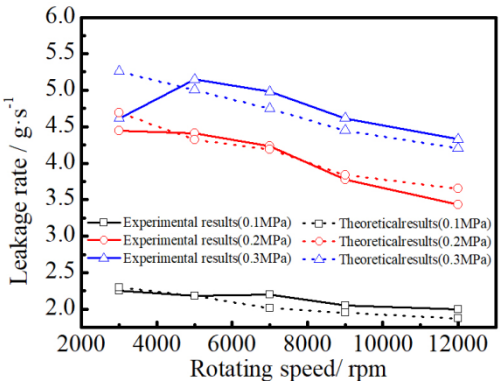

Figure 20. Comparison between theoretical results and experimental results

CONCLUSIONS

An innovative variable stiffness curve structure of finger seals is studied to resolve the contradiction between hysteresis and wear life of finger seals. A performance analysis model is established considering the initial installation condition of the finger seal to analyze the performances of the variable stiffness finger seal and traditional involute curved finger seal. Then, the experimental investigation of the variable stiffness finger seal is carried out.

According to the theoretical and experimental results, the following conclusions can be obtained:

1) Owing to the self-adaptive capacity of the variable stiffness structure, the variable stiffness finger seal can balance hysteresis and wear to achieve high synthetic performance. Compared with the traditional involute curved finger seal, the hysteresis characteristic of the variable stiffness finger seal under high speed is better. In addition, its hysteresis characteristic decreases with increase in rotating speed. Based on the predicted contact pressure, the wear performance of the variable stiffness finger seal is expected to be better at high pressure differential than the involute curved finger seal. Although, according to an incoordinate comparison on experimental results, the leakage rate of the variable stiffness finger seal is 1.5 to 2.0 times greater than the involute curved finger seal; but considering the difference on their structural parameters, it can be predict that the variable stiffness finger seal has a considerable or even better sealing performance under the similar structural and operating conditions. Therefore, under high speed and high pressure conditions, the variable stiffness finger seal exhibits considerably better sealing performance in terms of hysteresis and wear compared to the traditional involute curved finger seal.

2) It is necessary to consider the effect of initial installation condition for the performance analysis of the finger seal. The rationale of the established performance analysis model for the finger seal is verified through experimental results.

3) When the rotating speed of the rotor changes randomly, the hysteresis leakage of the variable stiffness finger seal is better than that of the traditional involute curved finger seal.

This is verified through theoretical analysis and dynamic leakage test results. Moreover, the durability test results of the variable stiffness finger seal indicate that it exhibits excellent dynamic operating stability.

ACKNOWLEDGMENTS

This work was supported by the National Natural Science Foundation of China (Grant No. 51305343).

DECLARATION OF INTERESTS

The authors declare no conflicts of interest with respect to the research, authorship, and publication of this article.

REFERENCES

1. Mackay, G and Wright E(1991). Laminated finger seal. U.S. Patent 5042823.
2. Proctor MP, Kumar A and Delgado IR. High-speed, high-temperature finger seal test results. *Journal of Propulsion & Power*, 2002, 20(2): pp. 312-318.
3. Liu TW and Zheng J. Experimental study on seal performance of finger seal. In: *Dynamic chapter of academic forum on a century aeronautics and astronautics by CSAA*, Beijing, China, 2003.
4. Proctor MP and Delgado IR(2004). Leakage and power loss test results for competing turbine engine seals. ***NASA/TM-2004-213049***.
5. Delgado IR and Proctor MP(2006). Continued investigation of leakage and power loss test results for competing turbine engine seals. ***AIAA-2006-4754***.
6. Chen GD, Xu H, Yu L, et al. Analysis to the hysteresis of finger seal. *Chinese Journal of Mechanical Engineering*, 2003, 39(5): pp. 121-124(in chinese).
7. Irebert R. Delgado, Margaret P. Proctor(2006). Continued Investigation of Leakage and Power Loss Test Results for Competing Turbine Engine Seals. ***AIAA-2006-4754***.
8. Gul K. Arora, Margaret P. Proctor, et al(1999). Pressure Balanced, Low Hysteresis, Finger Seal Test Results. ***AIAA-99-2686***.
9. Margaret P. Proctor, Irebert R. Delgado(2004). Leakage and Power Loss Test Results for Competing Turbine Engine Seals. ***GT2004-53935***.
10. Hendricks R.C, Bern O'Halloran, Gul K. Arora, et al(1994). Advances in Contacting Sealing. ***NASA CP-3282***.
11. Chen GD, Lu F, Yu QP, et al. Dynamic analysis of finger seal using equivalent model based on distributed mass method. *ARCHIVE Proceedings of the Institution of Mechanical Engineers Part C Journal of Mechanical Engineering Science*, 2014, 228(228): pp. 2992-3005.
12. Wang LN, Chen GD, Su H, et al. Effect of temperature on the dynamic performance of C/C composite finger seal. *Proceedings of the Institution of Mechanical Engineers Part G Journal of Aerospace Engineering*, 2016, 230(12): pp. 2249-2264.

13. Wang LN, Chen GD, Su H, et al. A transient performance analysis of finger seal considering compressed fluid in the leakage clearance. *Journal of Aerospace Power*, 2015, 30(8): pp. 2004-2010 (in chinese) .
14. Chen GD, Xu H, et al. On Selecting Proper Shape of Finger Seal. *Journal of Northwestern Polytechnical University*, 2002, 20(2): pp. 218-221(in chinese).
15. Wu YE, Chen GD and Lei YN. Engineering optimization design of shape-curve of finger-seal of aero-engine. *Journal of Northwestern Polytechnical University*, 2006, 24(2): pp. 260-264(in chinese).
16. Zhang YC, Chen GD, Shen XL. Performance Optimization for Finger Seal Based on Fuzzy Nash Equilibrium Game. *Journal of Aerospace Power*, 2010, 25(1): pp. 228-233(in chinese).
17. M.J. BRAUN, H.M. PIERSON and D. DENG. Thermofluids Considerations and the Dynamic Behavior of a Finger Seal Assembly. Tribology Transactions, 2005, 48(4): pp. 531-547.
18. M. J. Braun , H. M. Pierson and V. V. Kudriavtsev. Finger Seal Solid Modeling Design and Some Solid/Fluid Interaction Considerations. *Tribology Transactions*, 2003, 46(4): pp. 566-575.
19. Su H, Chen GD. Structural Optimization of Finger Seal Based on Conceptions of “Customized” and “Generalized” Finger Curves. *Acta Aeronautica et Astronautica Sinica*, 2007, 28(6): pp. 1506-1512(in chinese).
20. Li ES and Chen GD. Study on a new shape-curve of finger seal with low- hysteresis and low-wear. *Journal of Aerospace Power*, 2008, 23(4): pp. 759-764(in chinese).
21. Zhang YC, Chen GD, Shen XL. Analysis of Dynamic Performance and Leakage for Finger Seal. *Acta Aeronautica et Astronautica Sinica*, 2009, 30(11): pp. 2193-2199(in chinese).
22. Zhang YC. Performance Analysis and Optimization Research of Finger Seal. Xi'an, *Northwestern Polytechnical University*, 2009(in chinese).
23. Zhang YC , Liu K, Cui YC, Zhou CG. Optimization investigation on contact finger seal performances based on a fuzzy game approach, *Advances in Information Sciences and Service Sciences*, 2012, 4(15): pp. 375~381(EI)
24. Bai HL, Wang W, Zhang ZS, et al. Analysis of leakage flow of finger seal based on porous medium model. *Journal of Aerodynamics*, 2016, 31(6): pp. 1303-1308. (in chinese).

NOMENCLATURE

$y(t)$	displacement excitation of rotor
n	rotating speed of rotor, r/min
δ	radial clearance of supporting bearing, mm
n^*	critical rotating speed of rotor, r/min
k	number of time steps in one motion cycle
N_j	number of circular symmetrical structures in the j^{th} region
Δt	time step
T	motion cycle of rotor
β	leakage coefficient
Δp	pressure differential between upstream and downstream, MPa
ρ	density of sealed fluid
Δl	arc length of leakage clearance along the circumferential direction, mm
h_{ij}	height of leakage clearance at the i^{th} time step in the j^{th} region, mm
L	axial thickness of finger seal, mm
η	dynamic viscosity of sealed fluid, Pa.s

Table 1 Materials and physical performance parameters of the model

	Materials	Elastic modulus （$\times 10^{11}$Pa）	Poissonbies	Densities （g/cm^3）
Finger element	GH605	2.31	0.286	9.13
Forward cover plate	2Cr13	2.14	0.346	6.35
Rotor	40CrNiMoA	209	0.295	7.85

Table 2 Structural parameters of finger seal

Parameters	Symbol	Units	Involute	Variable stiffness
Radius of rotor	r	mm	40	40
Out radius of finger beam	r_w	mm	55	55
Clearance	d	mm	0.2	0.2
Height of finger feet	h	mm	0.7	0.4
Number of finger beams	m	--	42	42
Thickness of finger elements	t	mm	0.2	0.2
Root radius of finger beam	r_e	mm	48	48
Downstream protection height	h_x	mm	0.45	0.45
Radius of base circle	r_b	mm	0.008	--

Table 3 Average hysteresis rate and contact pressure of finger seal

Parameters	Involute	Variable stiffness
Hysteresis rate (%)	80.2	39.6
Average contact pressure (MPa)	0.5725	0.4386